15405 FINE-GRAINED IMPACT MELT (KREEP) ST. 6A 513.1 g

INTRODUCTION: 15405 is a fine-grained impact melt, of KREEP basalt composition and variolitic texture. It has a clast population limited to A15 KREEP basalts and quartz-monzodiorites ("QMD"), among the most rare-earth enriched of lunar samples, which are probably closely related to each other. Most radiogenic isotope systems of the QMD were disturbed ~0.6 to 1.2 b.y. ago, and possibly the impact melt was formed at that same time. Lead ages on zircons in QMD indicate an age of 4.37 b.y. (Compston et al. 1984).

15405 was the only rock sample collected at Station 6A, the highest location explored on the Apennine Front. It was chipped from the top of a distinctive isolated boulder which was sighted and identified as a sampling target en route to Station 6. The 3 m-long boulder has a prominent soil fillet in the upslope side and soil was present on top of the boulder: these greenish soils were also sampled.

The sample is blocky and angular, and extremely tough, with a medium gray to dark gray matrix (Figs. 1, 2). Although described as fractured in the Apollo 15 Lunar Sample Information Catalog (1974), it really resembles a block of a lava or welded slablets (Imbrium Consortium 1976; Marvin subsection p. 76). Although described in PET (1972) as closely resembling 15445 and 15455 from Spur Crater, 15405 is actually quite different in melt composition, texture, and clast population. It was originally studied cursorily in a Consortium headed by Murthy, and later studied by the Imbrium Consortium, whose reports are abbreviated below as ICR 1 (=1976) and ICR 2 (=1977).

PETROLOGY: The matrix, which makes up about 95% of the rock, is fine-grained and vesicular (Fig. 2). Mineral clasts and small (<l mm) light-colored lithic clasts are common; a few lithic clasts are up to 1 cm. An important type of clast is speckled black-and-white (Fig. 3), and is an igneous KREEP-rich quartz-monzodiorite. Slabbing of the rock shows many clasts to be strung out as schlieren, sometimes quite porous, and the sample exhibits flow banding and lenticular fissures (ICR 2, Marvin subsection, p. 19) (Fig. 2).

The petrography of the matrix and the clasts has been described by the Imbrium Consortium (ICR 1, subsections Marvin p. 76, Ryder and Bower p. 77, Taylor p. 94; and ICR 2, subsections Marvin p. 19, Ryder and Bower p. 20) and Ryder (1976). The matrix is an opaque, fine-grained, rather uniform, variolitic impact melt (Fig. 4) with a major and trace element composition similar to A15 KREEP basalts. It was classified as a subophitic impact melt by Simonds et al. (1975). It consists of plagioclase, pyroxene, and ilmenite laths with interstitial angular patches of glass. The melt texture does not define the foliation, which is instead defined only by some clast orientation and by the lenticular fissures and schlieren.

Figure 1. 15405,0 prior to sawcut in 1975; sawcut slab outlined. S-75-21518

Lithic clasts are of two main types: A15 KREEP basalts with a variety of textures (Fig. 5), and quartz-monzodiorites (QMD), a more silicic, coarser-grained lithology (Fig. 6). Other clasts, such as granitic fragments (Ryder 1976) and Fe-metal rich fragments(ICR 2, Ryder and Bower subsection, p. 20) appear to be unrepresentative fragments of quartz-monzodiorite or at least closely related to them. The only other lithic clast-type identified in thin sections is a single small olivine-vitrophyric melt-rock (Fig. 4). Other rock types such as mare basalts, anorthosites, breccias, or glass are conspicuously absent. Virtually all the individual mineral fragments in the matrix are pyroxenes and plagioclases derived from A15 KREEP basalts or quartz-monzodiorites (Fig. 8).

Figure 2. Subdivisions of slab 15405,95. Prominent white clasts are quartz-monzodiorite. S-76-24833

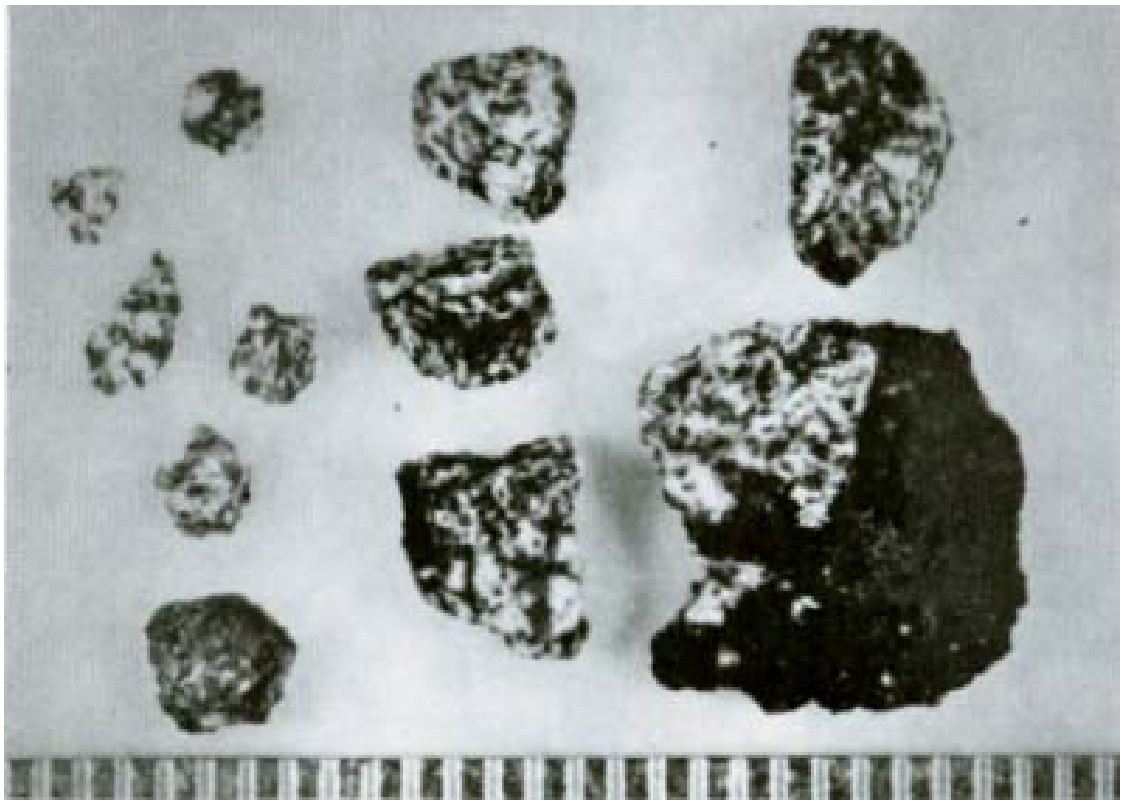
Figure 3. Quartz-monzodiorite clast A fragments. Scale is millimeters.

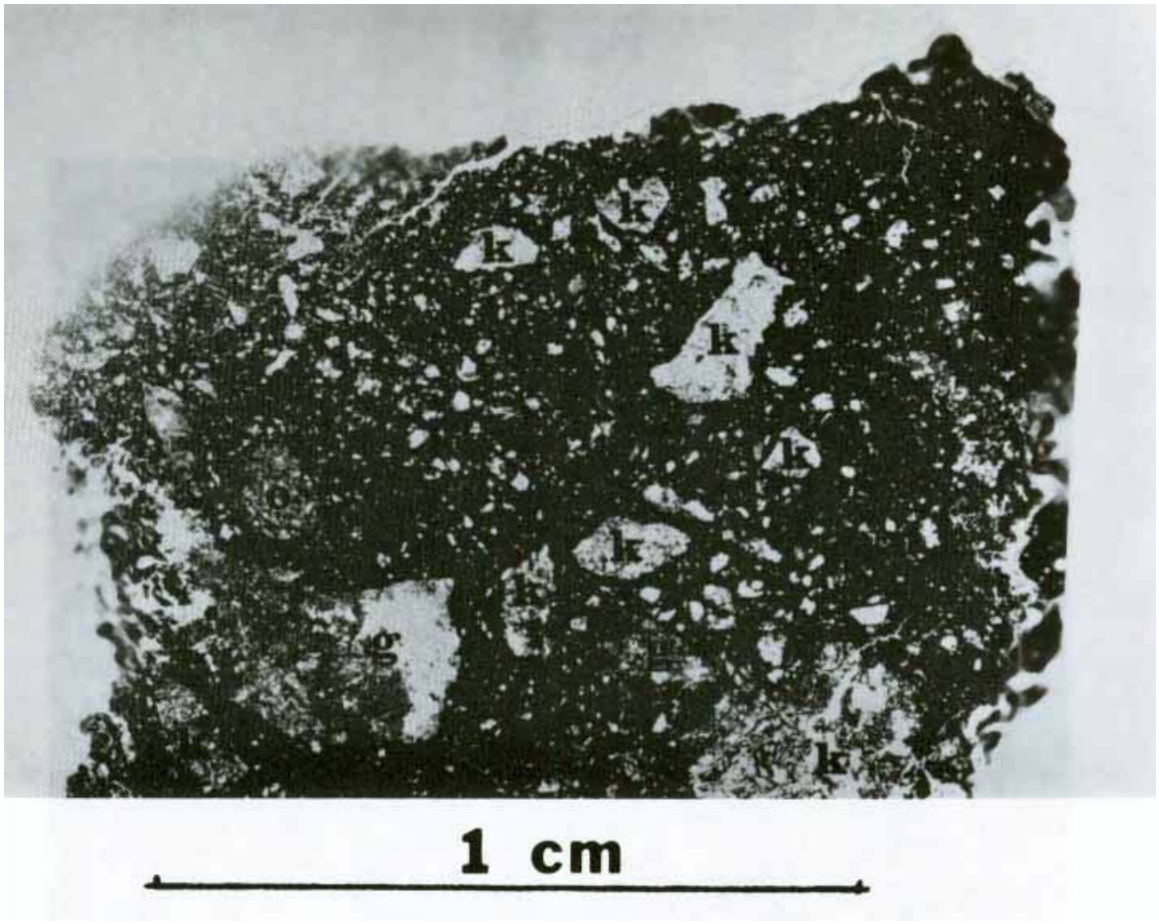

Fig. 4a

Figure 4. Photomicrographs of matrix of 15405.
a) whole thin section 15405,12, transmitted light. K = KREEP basalt, g = QMD ("granite"), o = olivine-vitrophyre.
b) 15405,11, transmitted light,
c) melt matrix, 15405,11. Reflected light.

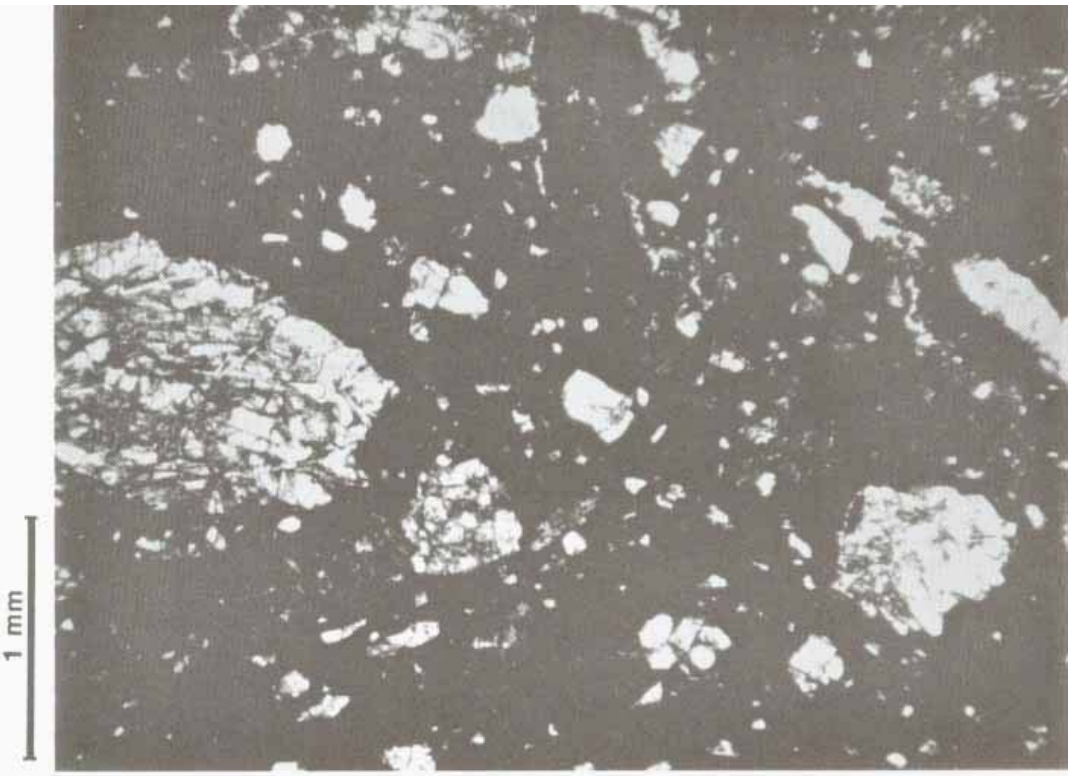

Fig. 4b

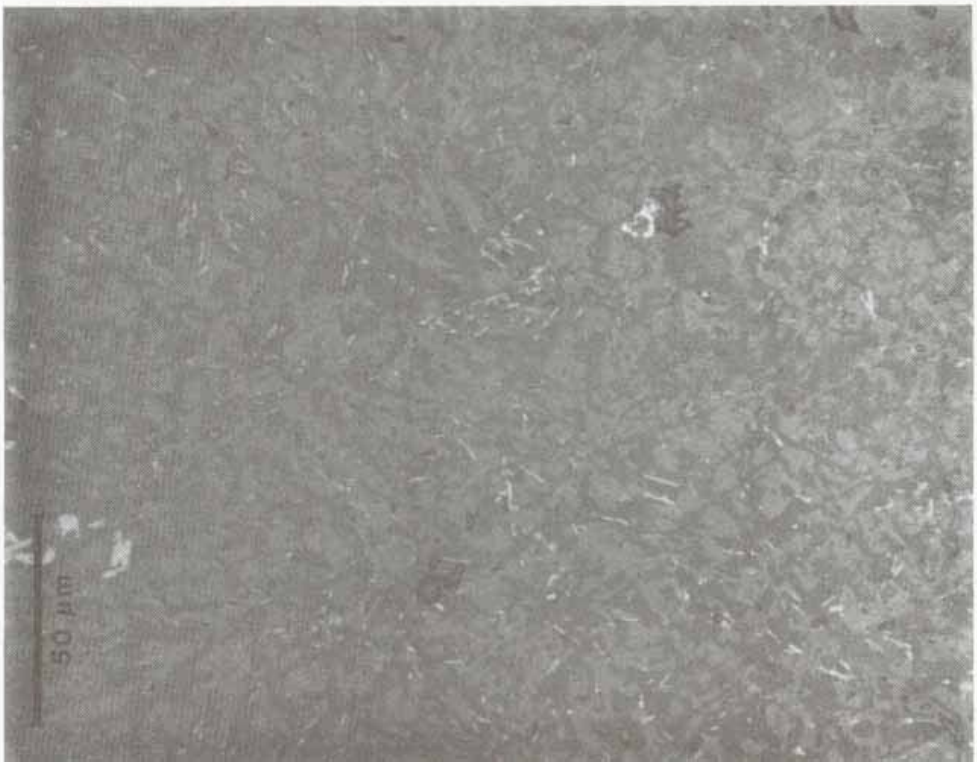

Fig. 4c

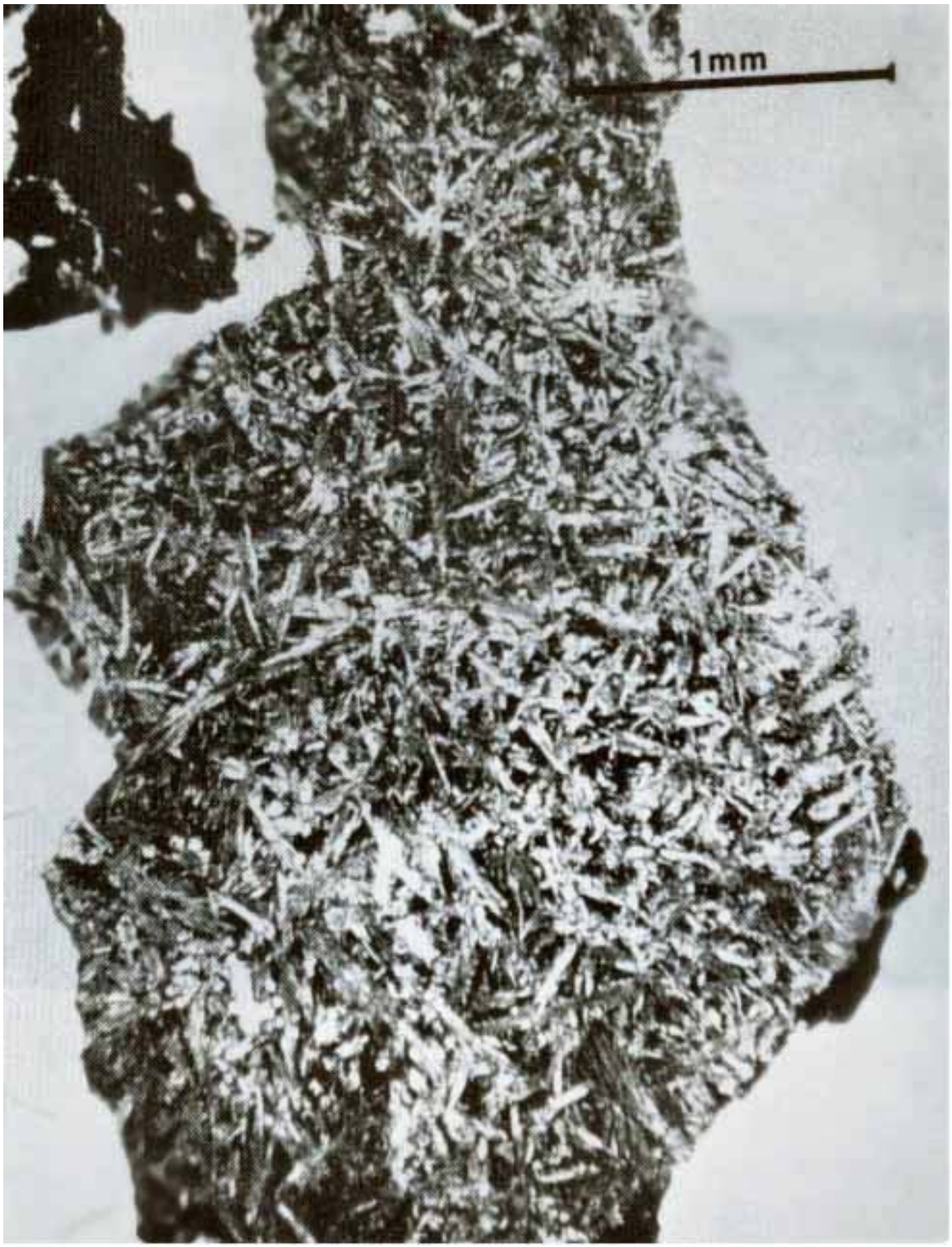

Fig 5a.

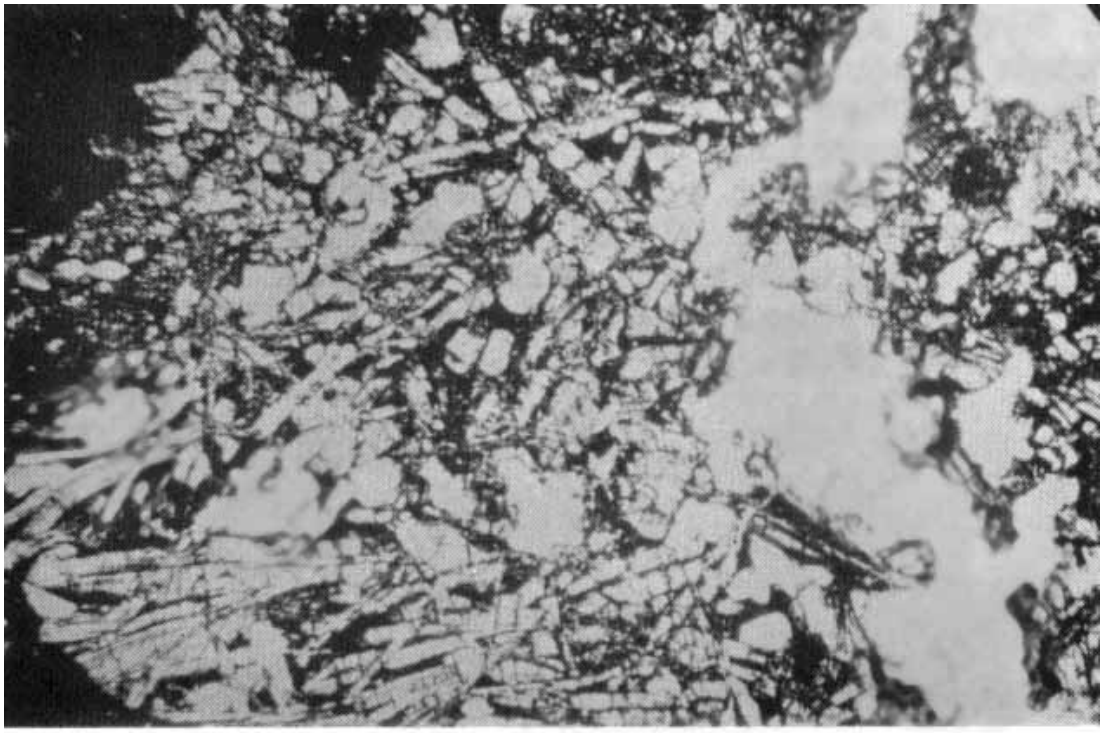

Fig. 5b

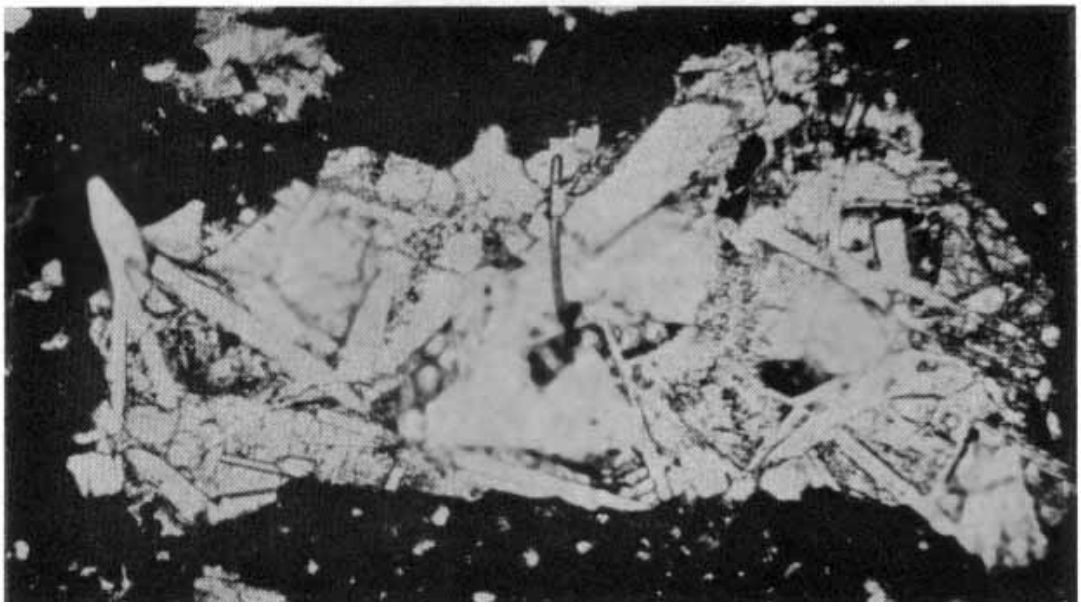

Fig. 5c

Figure 5. Photomicrographs of KREEP basalt clasts, all to same scale, transmitted light.

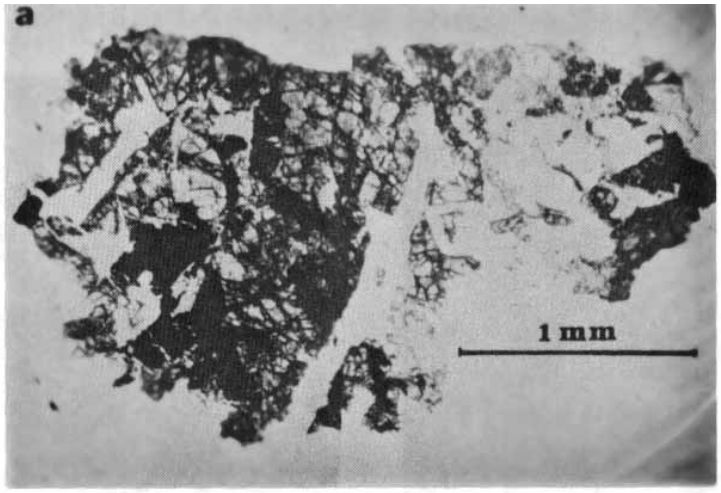

Fig. 6a

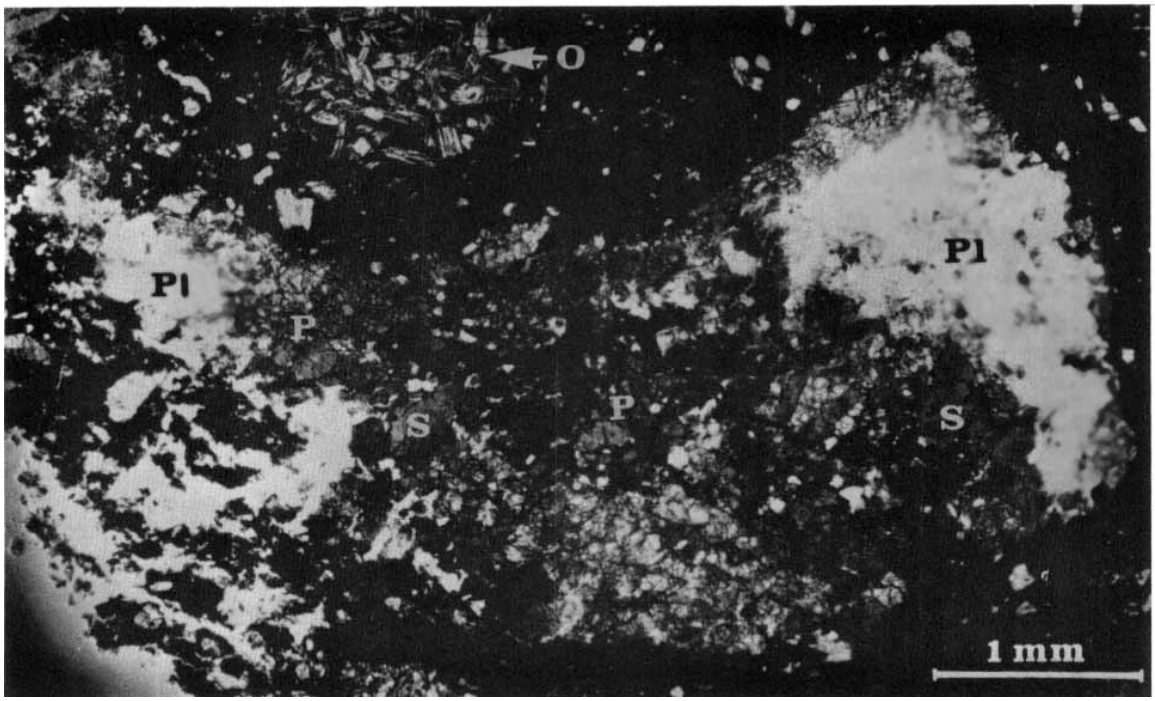

Figure 6. General photomicrographs of QMD.
a) 15405,56, whole thin section, transmitted light,
b) fragment in 15405,12 ("granite").
S = silica phase, P1 = plagioclase, P = pyroxene, O = olivine-vitrophyre

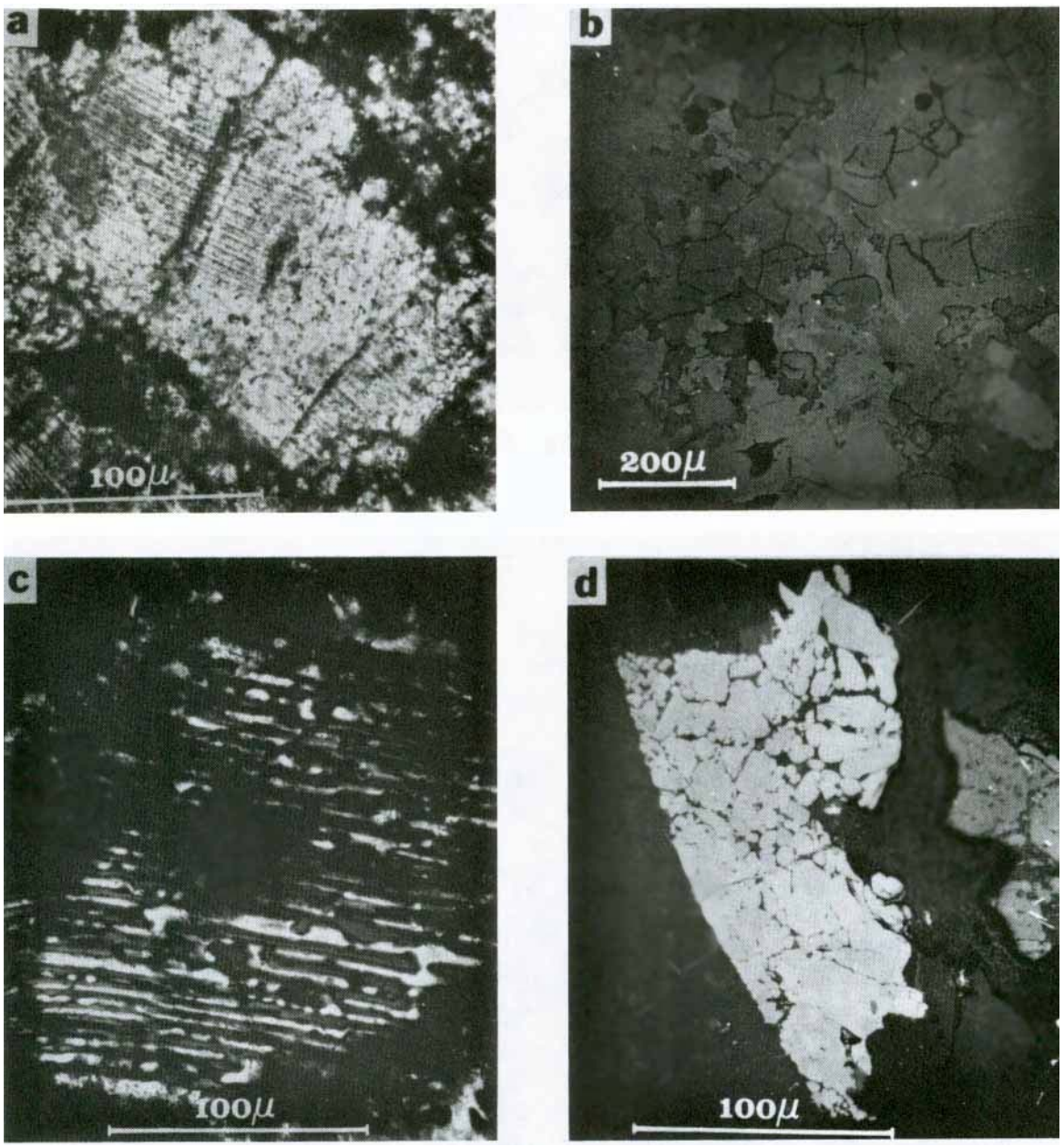

Figure 7. Photomicrographs of phases in QMD.
a) exsolved ferroaugite (transmitted light);
b) silica (dark gray with curved fractures), plagioclase (dark gray), and pyroxene (light gray) (reflected light);
c) silica-potassium feldspar intergrowth (crossed polarizers);
d) ilmenite (bright) with Si-K fine-grained mesostasis (reflected light).

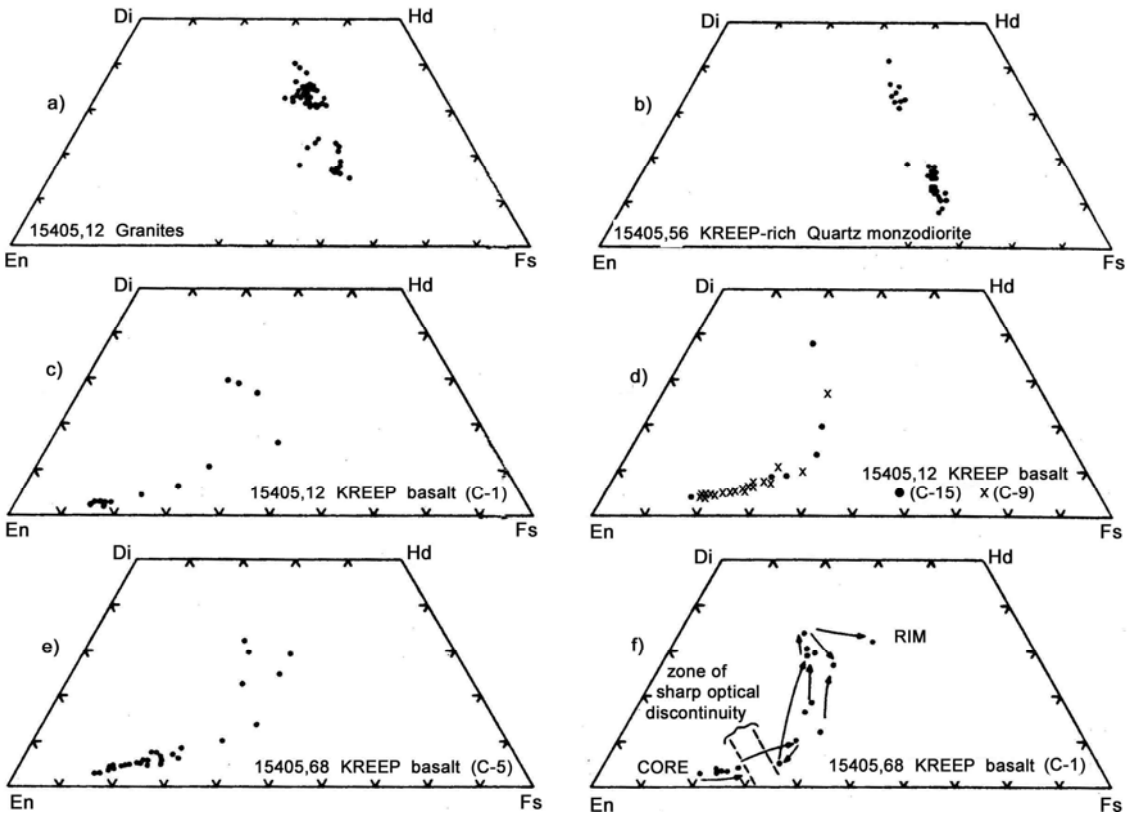

Figure 8. Compositions of pyroxenes in 15405 clasts.

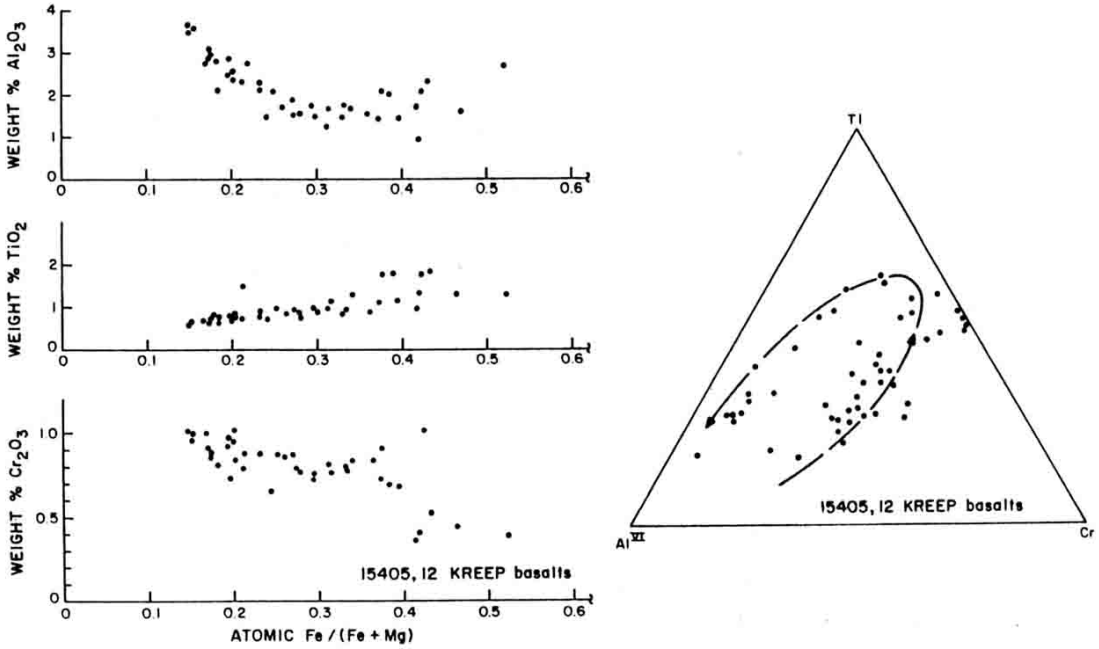

Figure 9. Minor elements in pyroxenes in 15405 KREEP basalts.

The KREEP basalt fragments are described by the Imbrium Consortium (ICR 1, Ryder and Bower subsection, p. 77) and, briefly, by Ryder (1976). They are texturally and mineralogically similar to other A15 KREEP basalts (Figs. 5, 8, 9, 11). They have a wide range of textures and grain-sizes, and consist mainly of plagioclase, zoned pyroxenes, and interstitial phases including cristobalite, ilmenite, phosphates, iron metal, and glass. Two small crystals of Mg-olivine have been identified in these basalts.

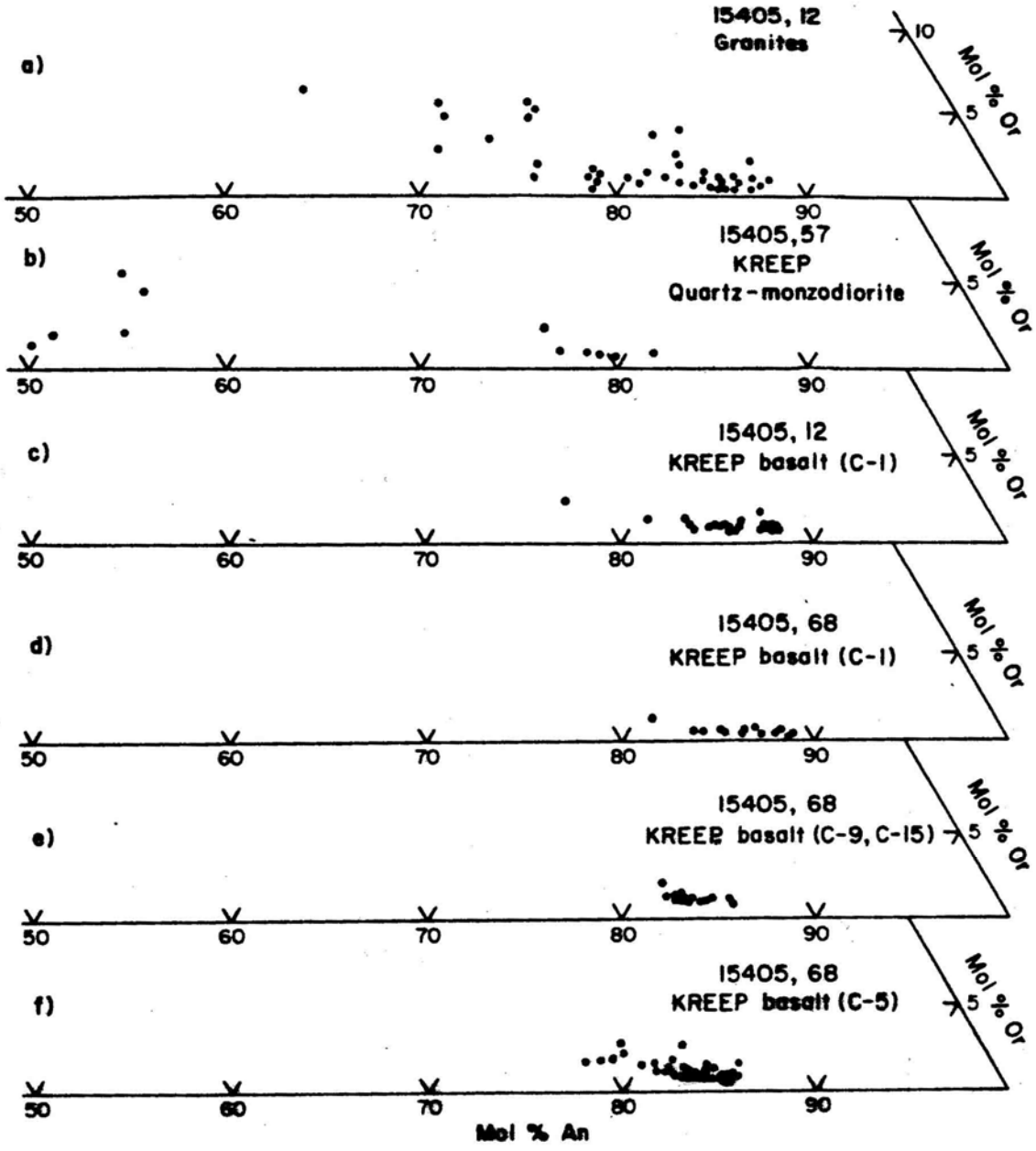

Figure 10. Minor elements in pyroxenes in 15405 QMD.

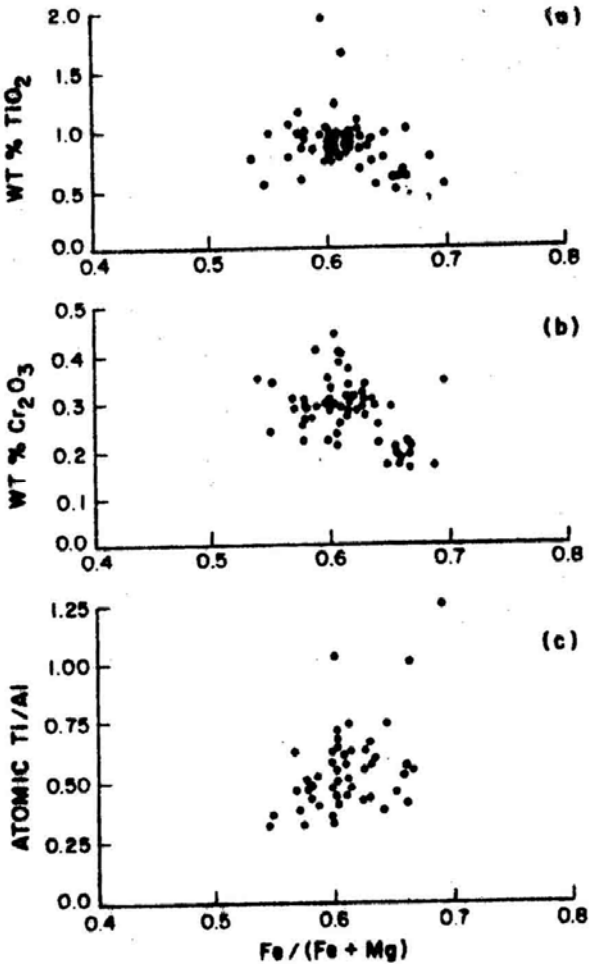

Figure 11. Compositions of plagioclases in 15405.

The quartzmonzodiorite clasts (Ryder 1976; G. Taylor et al. 1980; ICR 1, ICR 2), are less abundant than KREEP basalt clasts, but tend to be larger (e.g. Fig. 3). They tend to be more brecciated than the basalts (Fig. 6b); those with a better preserved texture are coarse basaltic, with plagioclase laths. However, they are not just coarse KREEP basalts--they have much more cristobalite and potash feldspar, have more equilibrated and iron-rich exsolved pyroxenes, and have plagioclase which is more sodic (Figs. 6, 7, 8, 10, and 11). The silica and potash feldspar phases are intergrown (Fig. 7c). Zircon, phosphate, and ilmenite are prominent, and fayalite and Fe-metal are present in some fragments. The mineral compositions (analyses or analysis plots in Ryder, 1976; G. Taylor et al, 1980; Takeda et al, 1981; and ICR 1, ICR 2) are similar to those in the end-products of KREEP basalt crystallization. G. Taylor et al. (1980) estimate a mode of ~35% each of pyroxene and plagioclase, 10-15% each of silica and potash feldspar, ~0.5 to 1.0% each of zircon, ilmenite, whitlockite, and minor chromite and Fe-metal (<0.02% Ni, 0.2% Co). Zircon chemical data is provided by Compston et al. (1984). The distinction originally made between "granites" and quartzmonzodiorites (Ryder, 1976) is probably not real, as the

two types have identical mineral compositions; the "granites" are probably unrepresentative fragments of quartzmonzodiorites (ICR 2, Ryder and Bower subsection, p. 20).

The quartzmonzodiorites were deformed by shock and shock heating, disturbing the radiogenic isotope systems (below) and even melting pyroxenes in places (Takeda et al., 1981). Takeda et al. (1981) studied the composition, exsolution, inversion, and deformation of the pyroxenes using analytical TEM, single-crystal XRD, and microprobe techniques. In agreement with previous workers, Takeda et al. (1981) found that the quartzmonzodiorites contain two pyroxenes--a pigeonite and a subcalcic augite--each exsolved. Individual grains are homogeneous (except for exsolution) but there are slight differences among grains. Deformation is heterogeneous, and includes mechanical twinning, dislocations, and shock-heat-produced melting.

Ryder (1976), Nyquist et al. (1977), and Irving (1977b) suggested that QMD formed by fractional crystallization of a KREEP basalt magma. In contrast, Rutherford et al. (1976) suggested that silicate liquid immiscibility also played a part. This possibility was discussed by Ryder (1976) and G. Taylor et al. (1980) who found the chemical evidence to be largely against immiscibility. Ryder (1976) suggested a close relationship between the QMD and the KREEP basalt fragments in 15405 because of the chemical similarities and lack of other kinds of fragments in the samples.

CHEMISTRY: Analyses of matrix or bulk rock are listed in Table 1, and of clasts (mainly QMD) in Table 2. Rare earths for all analyzed lithologies are plotted in Figure 12. Table 3 lists microprobe-derived analyses of matrix and QMD.

The matrix/bulk rock has major and incompatible element abundances very like those of pristine KREEP basalts 15382 and 15386, and is presumably mainly derived from material like the KREEP basalt clasts within the matrix. There are discrepancies among analyses, probably resulting in part from varied clastic materials among splits, and in part from small sample sizes. The analysis by Laul and Schmitt (1972, 1973) of sawdust produced during rock processing has high MgO (and, by difference, low SiO_2) and is perhaps less reliable than other analyses. The matrix has siderophile element abundances elevated over those of pristine KREEP basalts (e.g., Ir ~l ppb) indicating meteoritic contamination, but at rather low levels cf. most highlands breccias (Ir 5-10 ppb). The two different splits analyzed by Anders' group were assigned to separate projectile groups (2 and 3H; Hertogen et al., 1977) on siderophile ratios.

KREEP basalt clasts were only specifically analyzed in bulk with microprobe defocussed beam (Ryder and Bower, ICR 1) but the white clast fragment (A-1) analyzed by Ganapathy et al. (1973) has trace elements (Table 2) similar to the matrix and KREEP basalts rather than to QMD. While the Ir abundance (0.343 ppb) of the clast is non-pristine, it is very low and the sample was not assigned to any meteoritic projectile group (Hertogen et al., 1977). The remaining analyses in Table 2 are specifically of QMD fragments. These analyses demonstrate the evolved nature (Mg ~0.35; light REEs 500 to 700 x chondrites, among the highest reported for lunar samples) which lead to QMD

being dubbed "super-KREEP" by Nyquist et al. (1977; ICR 2). The QMD is nearly uniformly enriched in REE abundances relative to the 15405 matrix, except for a deeper Eu anomaly. The analyses are quite consistent given the coarse grain size, and are consistent with the Nyquist et al. (ICR 2) contention that the high rare earth abundances well-represent bulk rock and do not result from an unrepresentative overabundance of some exotic mineral such as whitlockite. Siderophile element abundances demonstrate a lack of meteoritic contamination, and there is no doubt that QMD is an igneous rock type. Its major element composition places the lithology close to the Qz-Plag-Px eutectic in the Silica- Forsterite-Anorthite system. Nyquist et al. (1977, ICR 2) found the major and trace element abundances to be consistent with an origin by ~64% crystallization of KREEP basalt or by 34% partial melting of a KREEP basalt (quartz-normative) source, and that immiscibility is not involved in the petrogenesis, a conclusion also reached by G. Taylor et al. (1980).

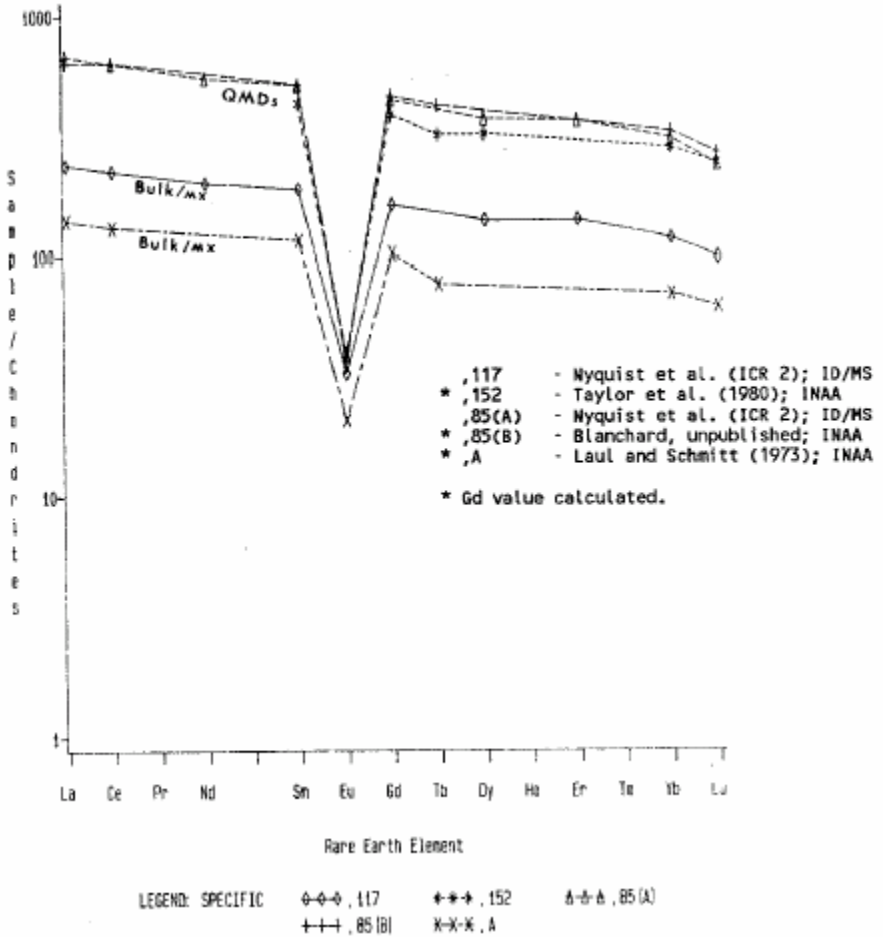

Figure 12. Rare earths in 15405 bulk rock/matrix, and QMD fragments.

TABLE 15405-1. Chemical analyses of bulk rock or matrix

		a	,5,A-5	,26	,63	,62	,59	,49	,117
Wt %	SiO2			51.49					
	TiO2	1.2		1.80					
	Al2O3	13.8		15.44					
	FeO	12.8		11.17					
	MgO	14		7.33					
	CaO	10.3		9.98				7.6	
	Na2O	0.547		0.81					
	K2O	0.40		0.82				1.4	0.7120
	P2O5		0.72		0.57				
(ppm)	Sc	23		23					
	V	91		22					
	Cr	2050		1500					
	Mn	1420		1500					
	Co	36		9.8					
	Ni			43	83				
	Rb		25.6	29	27.4				20.5
	Sr			190					168
	Y			360					
	Zr	500		1100					
	Nb			80					
	Hf	16.2							
	Ba	480		1200					767
	Th	10					16.2		
	U	2.3	5.105		4.690	3.1	3.93		
	Pb			6.0			9.64		
	La	46		55					78.7
	Ce	114							197
	Pr								
	Nd								120
	Sm	20.9							34.2
	Eu	1.45							2.27
	Gd								40.3
	Tb	3.6							
	Dy								44.2
	Ho								
	Er								28.0
	Tm								
	Yb	14		32					23.5
	Lu	2.1							3.32
	Li			24					36.8
	Be			9.7					
	B								
	C								
	N								
	S								
	F								
	Cl					53.3			
	Br		0.140		0.129	0.223			
	Cu			6.8					
	Zn		4.1	4.1	4.2				
(ppb)	I					0.6			
	At								
	Ga			4000					
	Ge		94		62.6				
	As								
	Se		89		78				
	Mo								
	Tc								
	Ru								
	Rh								
	Pd				1.7				
	Ag		2.9		2.22				
	Cd		16		17.7				
	In		1.0		1.47				
	Sn								
	Sb		0.81		1.06				
	Te		2.2		4.9				
	Cs		1160		1120				
	Ta	2000							
	W								
	Re		0.147		0.121				
	Os				1.16				
	Ir		1.64		1.28				
	Pt								
	Au		0.93		0.525				
	Hg				3.4				
	Tl		4.3		0.25				
	Bi		0.19						
		(1)	(2)	(3)	(4)	(5)	(6)	(7)	(9)

TABLE 15405-2. Chemical analyses of clasts

		,5,A-1	,86	,88(WRI)	,90	,87d	,85	,85	,152
Wt %	SiO2								(55.4)e
	TiO2								2.6
	Al2O3								11.9
	FeO							15.1	14.1
	MgO								3.8
	CaO				6.4				8.9
	Na2O							0.87	0.81
	K2O				2.8		1.71	1.8	2.1
	P2O5								
(ppm)	Sc							30.7	29
	V								33
	Cr							1220	1510
	Mn								1400
	Co							7.8	8.0
	Ni		<2						
	Rb	20.7	39.0			35.89	40.6		
	Sr					190.1	154		
	Y								
	Zr								1620
	Nb								
	Hf							51	44.7
	Ba						1490		1900
	Th			85.8				43	39.4
	U	4.105	11.500	17.4					11.1
	Pb			14.0					
	La						224	210	
	Ce						555	560	
	Pr								
	Nd						328		
	Sm						92.0	93	77.4
	Eu						2.69	2.52	2.75
	Gd						110		
	Tb							19.7	14.9
	Dy						116		101
	Ho								
	Er						71.7		
	Tm								
	Yb						60.9	65	55.2
	Lu						8.06	9.0	8.2
	Li						40.9		
	Be								
	B								
	C								
	N								
	S								
	F								
	Cl								
	Br	0.120	0.220						
	Cu								
	Zn	4.9	6.3					60	
(ppb)	I								
	At								
	Ga								
	Ge	160	345						
	As								
	Se	104	89						
	Mo								
	Tc								
	Ru								
	Rh								
	Pd		<0.9						
	Ag	2.5	2.15						
	Cd	9.8	18.9						
	In	1.0	45.2c						
	Sb	0.35	1.40						
	Te	1.9	9.4						
	Cs	920b	1190					1100	
	Ta							13,000	10,100
	W								
	Re	0.059	0.046						
	Os		0.007						
	Ir	0.343	0.0060						
	Pt								
	Au	0.25	0.051						
	Hg								
	Tl	3.7	5.8						
	Bi	0.21	0.31						
		(2)	(4)	(6)	(7)	(8)	(9)	(10)	(11)

References and methods for Tables 1 and 2:

(1) Laul and Schmitt (1973); INAA
(2) Ganapathy et al. (1973); RNAA
(3) Christian et al. (1976); XRF, etc.
(4) Gros et al. (ICR 1, 1976)
(5) Jovanovic and Reed (ICR 1, 1976); leaching; INAA
(6) Tatsumoto and Unruh (ICR 1, 1976); ID/MS
(7) Bernatowicz et al. (1978); argon isotopes
(8) Nyquist et al. (ICR 1); ID/MS
(9) Nyquist et al. (ICR 2); ID/MS
(10) Blanchard, unpublished; INAA
(11) Taylor et al. (1980); INAA

Notes:

(a) sawdust
(b) corrected value from Higuchi et al. (1975)
(c) doubtful value, contamination ?
(d) less than 44 micron fraction after grinding and sieving
(e) SiO2 by difference

TABLE 15405-3. Microprobe analyses of matrix and QMD in 15405

			Ts,12
Wt %	SiO2	57.4	49.7
	TiO2	1.1	1.6
	Al2O3	13.2	14.6
	FeO	11.2	10.7
	MgO	3.4	8.3
	CaO	9.0	11.8
	Na2O	1.0	0.84
	K2O	1.9	0.67
	P2O5	0.4	0.54
ppm	Cr		4300
	Mn		1200
	Zr	3000	
	Ba		1400
	La	183	
	Ce	413	
	Nd	287	
		(1)	(2)

References and methods:
(1) Ryder (1976); microprobe defocussed beam
(2) Taylor (ICR 1); mode/microprobe

STABLE ISOTOPES: Clayton et al. (1973) analyzed the oxygen isotopic composition of a matrix sample and a clast from 15405. The $\delta^{18}O$ of the matrix is 5.70%, of the clast is 6.0%. The clast is described as a "shocked troctolite with a salt-and pepper appearance" and is almost certainly in fact a quartz-monzodiorite sample. A sample specifically of quartz-monzodiorite analyzed by Clayton (ICR 2) gave a $\delta^{18}O$ of 5.68%, in no way exceptional for lunar rocks. The value demonstrates (by comparison with other lunar samples) that there is very little effect on the oxygen isotopic composition resulting from the igneous differentiation which produced acid rocks such as 15405 QMD and 12013.

GEOCHRONOLOGY AND RADIOGENIC ISOTOPES: The isotopic systems are generally disturbed, but indicate an age for the QMD greater than 4.0 b.y., likely greater than 4.2 b.y., and an age for the matrix melt of about 1 b.y. There is no indication of the 3.8 to 3.9 b.y. age which normally characterizes highlands breccias and A15 KREEP basalts.

Nyquist et al. (ICR l; ICR 2; 1977) reported Rb-Sr isotopic data for the quartz-monzodiorite, including mineral separates, and for the melt matrix. The quartz-monzodiorite separates show that the Sr is extremely radiogenic, but scatters, with no linear array defined (Fig. 13). This provides only loose constraints on chronology, the whole rock data corresponding with a model age of 5.3 b.y. demonstrating open-system behaviour for the rock as a whole. Because the Sr is so radiogenic, the model age should approximate the true age. Correcting for Rb loss by assuming original K/Rb ratios, Nyquist et al. (ICR 2; 1977) found that the whole rock age could not be older than 4.4 b.y., and for a typical Apollo 15 KREEP K/Rb, the age would be ~4.2 b.y. (Fig. 14). Younger ages cannot be excluded, but for the QMD and matrix to lie on a 3.9 b.y. isochron would require lower original K/Rb and greater Rb loss.

Bernatowicz et al. (ICR 2; 1977; 1978) attempted to date both the QMD and the matrix using the ^{40}Ar-^{39}Ar method. The QMD (,90) contains large amounts of trapped ^{36}Ar, which they believe to be a terrestrial atmospheric contamination. An intermediate temperature release plateau (800°-1100°C), in which 60% total ^{39}Ar was released, indicates a significant heating event at 1.29 ± 0.04 b.y. (Fig. 15a); there is however a large ^{40}Ar correction. The low temperature, low age may result from post-heating diffusion; the high temperature, high age may represent incomplete degassing of the QMD during the heating. For the matrix sample (,49) the correction for trapped ^{40}Ar is much more severe and precludes a clear age estimate. Qualitatively the releases are similar to those for the QMD, and in agreement with a 1.3 b.y. old heating event (Fig. 15b).

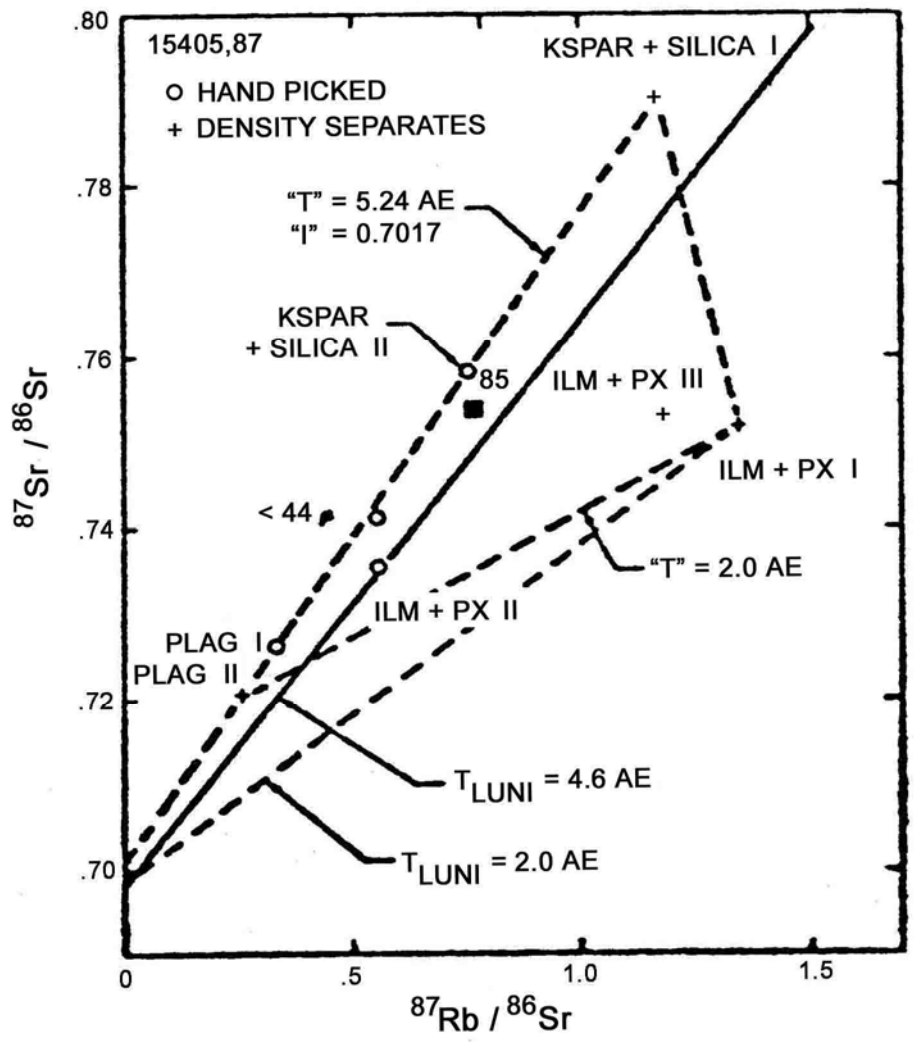

Figure 13. QMD Rb-Sr data
(Nyquist et al., 1977).

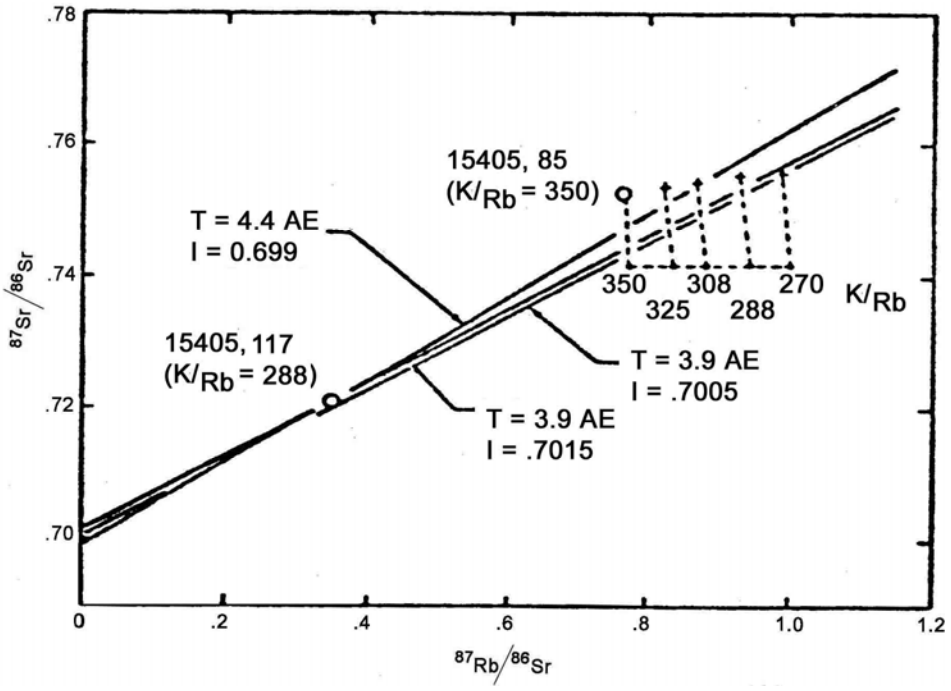

Figure 14. "Corrected" 15405 Rb-Sr isochron (Nyquist et al., 1977)

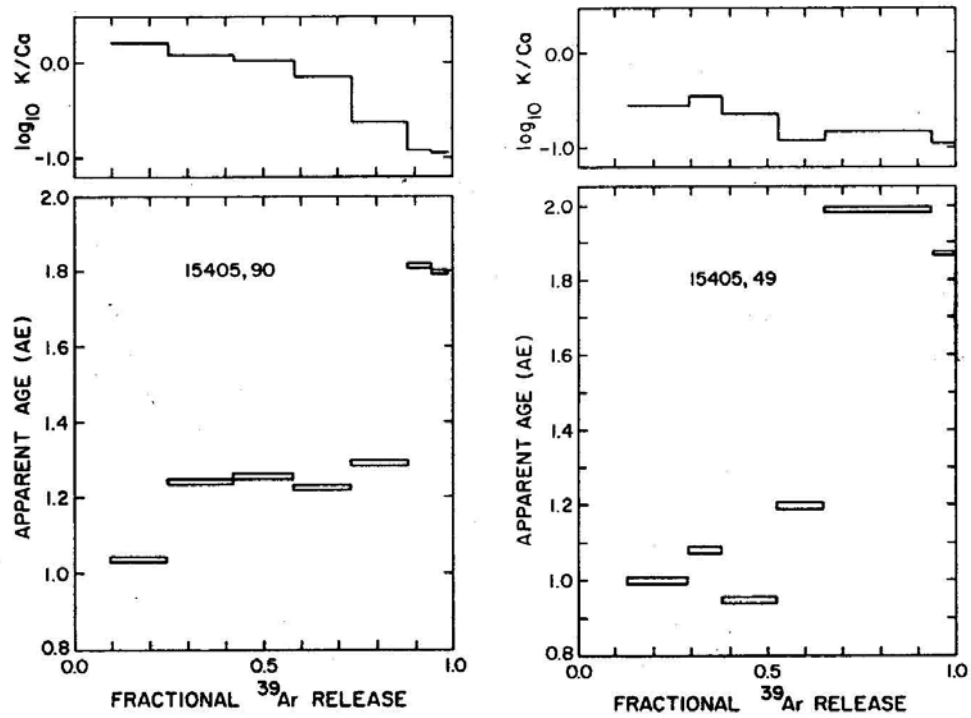

Fig. 15a

Fig. 15b

Figure 15. Ar release diagrams a) QMD ,90; b) matrix ,49 (Bernatowicz et al., ICR 2).

Tatsumoto and Unruh (ICR 1; 1976) and Unruh and Tatsumoto (1977) reported U, Th, and Pb isotopic data for whole rock and mineral separates of the QMD and for the matrix. The QMD contains the highest U and Th thus far analyzed for a lunar sample, and rather radiogenic Pb. The matrix is not so radiogenic and its U, Th, and Pb characteristics are typical of KREEP basalts. The U-Pb evolution (Fig. 16) demonstrates a complicated clast history with at least three events, including an event at 0.6 to 1.2 b.y. which disturbed the system. Making the assumption that U-Pb was closed during all but one of the recent disturbances leads to an age of 4.0 ± 0.1 b.y. for the QMD; this is merely a model age, with the additional disadvantage that it is poorly defined. A line joining the whole rock QMD and 15405 matrix points interceding concordia at ~4.2 and ~1.9 b.y. ago, substantially different from the "cataclysm" line characteristic of most highlands breccias.

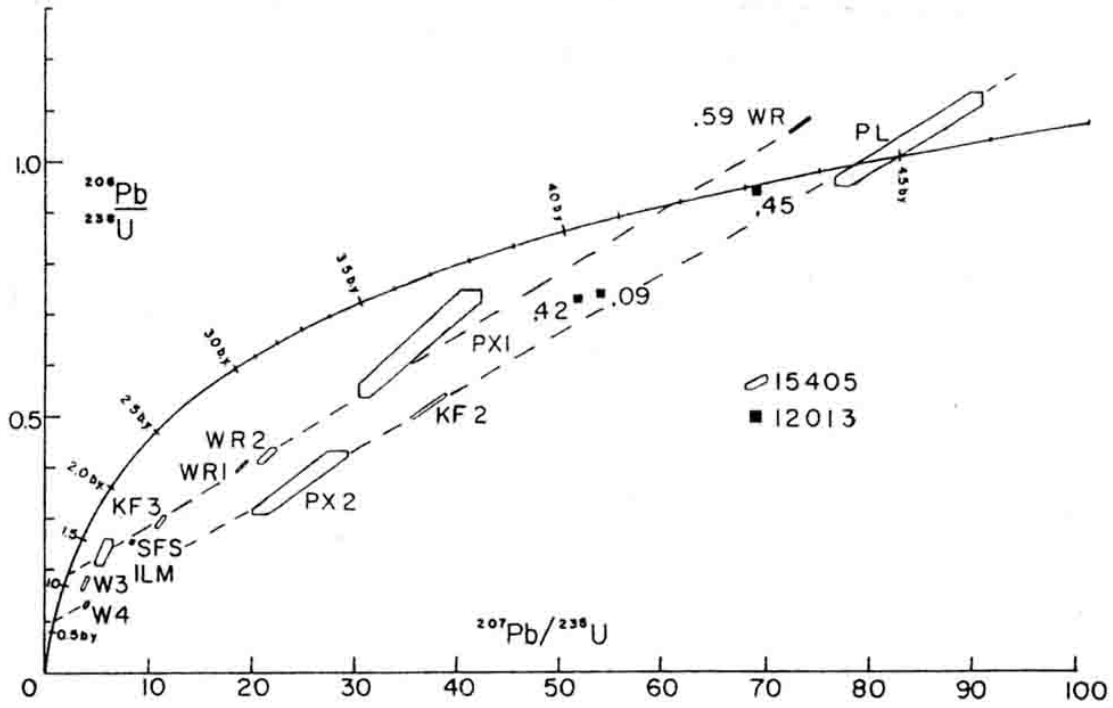

$^{206}Pb/^{238}U$ vs. $^{207}Pb/^{235}U$ evolution diagram for mineral separates and whole-rock analyses of 15405,88 and a whole-rock analysis of 15405.59. The data are corrected for meteorite primordial Pb ($^{206}Pb/^{204}Pb = 9.307$, $^{207}Pb/^{204}Pb = 10.294$; Tatsumoto *et al.*, 1973) so the upper concordia intercepts of the broken lines do not have any age significance. The lower intercepts and the scatter in the data indicate a young event (or events) of about 0.6–1.2 b.y. WR1 plots in a different place than previously reported in our abstracts (Tatsumoto and Unruh, 1976; Unruh and Tatsumoto, 1976) due to an erroneously calculated Pb concentration. Hexagons correspond to the calculated uncertainties for the data.

Figure 16. U-Pb evolution for 15405 materials (Tatsumoto and Unruh, 1976).

Compston et al. (1984) used a high resolution microprobe (SHRIMP) to analyze U,Th, and Pb in four zircon grains for the QMD. One is strongly discordant (60% Pb loss), the remainder vary from a few percent to 25% Pb loss. The locus of loss corresponds to an event at 1.4 b.y. Extrapolation to concordia gives an intersection at 4.365 ± .030 b.y., and one spot in one zircon contained Pb which can be interpreted as signifying the presence of a significantly older inclusion within the zircon. Highly radiogenic Pb was also found in plagioclase. As with the other isotopic systems, there is no record of the 3.8 or 3.9 b.y. event common to most highland breccias.

Podosek and Walker (ICR 1) found that fission tracks in a whitlockite in a chip of QMD correspond with a heating event 0.5 to 1.5 b.y. ago.

RARE GAS, TRACKS, AND EXPOSURE: Drozd et al. (1976) and Podosek and Walker (ICR 1) reported Ne, Kr, and Xe isotopic ratios for one matrix sample. The ^{21}Ne exposure age is 6 m.y., that of ^{81}Kr is 11.4 ± 1.1 m.y. The sample does not contain fission xenon in excess of that expected from in situ decay of ^{238}U and ^{244}Pu, and does not contain large amounts of solar wind gas. Bernatowicz et al. (1977, 1978) reported Ar isotopic ratios and abundances for samples of matrix and a QMD clast for varied temperature releases (see GEOCHRONOLOGY section).

Fleischer and Hart (1972, 1973) measured track density, track stability, and U in a matrix sample. Pyroxene and feldspar have an average density of (2.82 ± 0.54) x 10^5 tracks per cm^2. Most grains are distorted and this density is for undistorted areas. The density is low indicating a brief surface residence time--equivalent of 5 to 6 m.y. at 6 cm depth and 0.5 to 0.6 m.y. at 1 cm deep. Podosek and Walker (ICR 1) also measured tracks in a matrix sample, finding an approximately 10 m.y. surface exposure age.

PROCESSING AND SUBDIVISIONS: Early subdivision was made from loose and chipped pieces (Fig. 17). The 38.5 g chip ,5 was allocated to Murthy for consortium study; sawdust from its subdivision by Murthy was used by Laul and Schmitt (1972, 1973). Thin sections (,2, 3, 10-,16) were made from fragment ,1.

Subdivisions for the Imbrium Consortium are documented by Marvin (ICR 1, ICR 2), and included chipping ,0 and picking from ,8, a collection of chips and fines, for matrix, exterior surface, and quartz-monzodiorite separations. Subsequently the main piece ,0 was sawn (Figs. 1, 2) to produce slab ,95, from which many allocations were made. A summary of all the thin sections cut from 15405 is shown in Table 4.

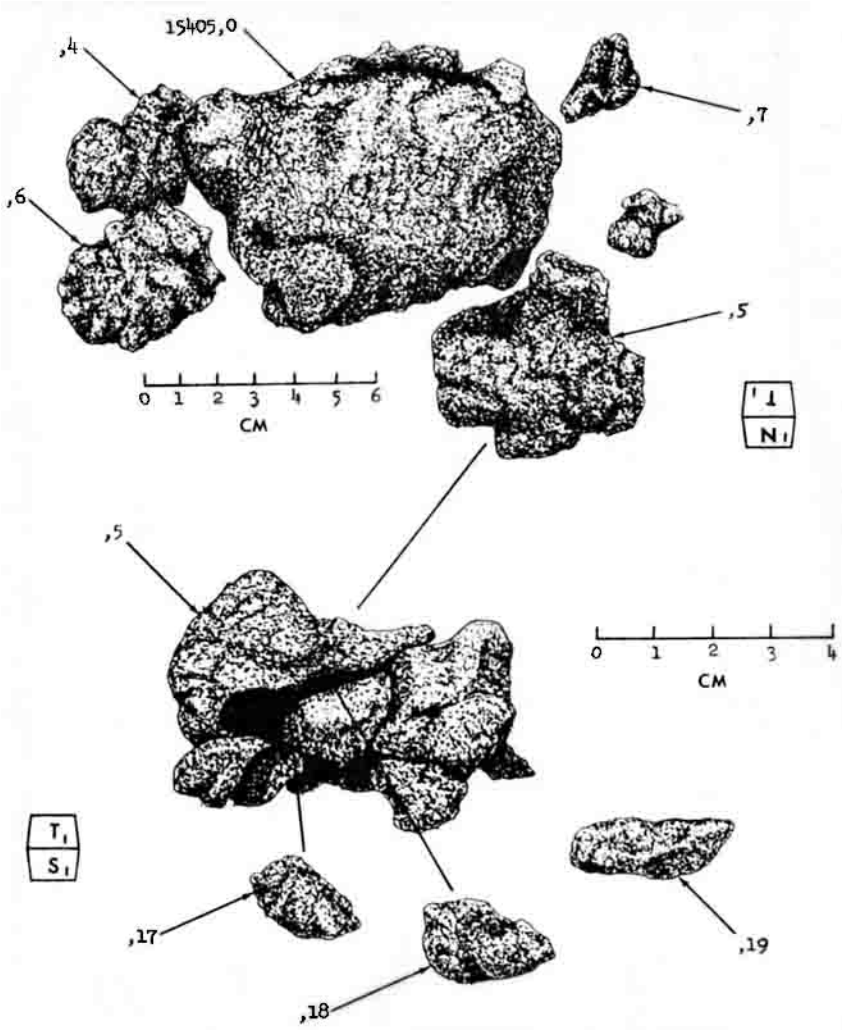

Figure 17. Original splitting of 15405.

TABLE 15405-4. Thin sections of 15405

NUMBER	LINEAGE AND PARENTAGE	DESCRIPTION
,2 ,3 ,10-,16	,1 ⟵ ,0	matrix and clasts
,33 ,34 ,35	,29 ⟵ ,6	matrix and clasts
,54 ,55	,50 ⟵ ,8 ⟵ ,0	matrix and clasts
,56 ,57	,52 ⟵ ,8 ⟵ ,0	quarzmonzodiorite
,68 ,69 ,70	,61 ⟵ ,7 ⟵ ,0	matrix and clasts
,145 ,146 ,147	,138 ⟵ ,95 ⟵ ,0	matrix and clasts. ,145 contains QMD
,166	,86 ⟵ ,6 ⟵ ,0	quartzmonzodiorite